RSC Advances

ROYAL SOCIETY OF CHEMISTRY

www.rsc.org/advances

Stability and deactivation of Fe-ZSM-5 zeolite catalyst for catalytic wet peroxide oxidation of phenol in a membrane reactor

Songshan Jiang, Huiping Zhang, Ying Yan, Xinya Zhang*

**School of Chemistry and Chemical Engineering, South China University of Technology, Guangzhou 510640, PR China*

Abstract

Stability and deactivation of Fe-ZSM-5 zeolite catalyst for catalytic wet peroxide oxidation (CWPO) of phenol were studied in a membrane reactor. Firstly, the Fe-ZSM-5 zeolite membrane catalyst was prepared by paper-making/sintering process, secondary growth process and incipient wetness impregnation method. And the influence of residence time on the CWPO of phenol was evaluated by modifying the catalyst bed height. Then, stability of the Fe-ZSM-5 zeolite membrane catalyst was studied by the long-term experiment (40 hours). Finally, the deactivation mechanisms of the Fe-ZSM-5 zeolite membrane catalyst were investigated by N_2 adsorption-desorption, X-ray diffraction (XRD), Filed emission scanning electron microscopy (FE-SEM), Thermal gravimetric (TG) analysis, Fourier transform infrared (FT-IR) spectra and Raman spectra, respectively. The results of CWPO of phenol showed that complete phenol conversion with a high TOC conversion (about 60%) was obtained at the catalyst bed height of 4 cm. Meanwhile, good stability with low Fe leaching concentration (about 0.5 mg/L) and high phenol conversion (above 85%) were obtained after continuously ran for 40 hours. Furthermore, the loss of active component, the partial phase change of Fe_2O_3, the crystalline change of ZSM-5 zeolite membrane and the coke formations on the surface of the catalyst were found to be responsible for the deactivation of the catalyst.

Keywords: Phenol; Catalytic wet peroxide oxidation; Fe-ZSM-5 zeolite membrane catalyst; membrane reactor; deactivation mechanism

* Corresponding author: Tel: +86 2087112047; fax: +86 2087112047.
E-mail address: cexyzh@scut.edu.cn (X.Y. Zhang).

1. Introduction

Catalytic wet peroxide oxidation process is an attractive catalytic approach aimed at deep oxidation of organic water pollutants with hydroxyl and hydroperoxyl radicals produced by decomposition of H_2O_2 in the presence of a catalyst under mild conditions (0.1-0.5 MPa, T≤100 ℃) [1, 2]. The heterogeneous CWPO process can overcome the disadvantages of homogeneous CWPO process such as the sensibility to pH (always within the range of 2.3-3.5) and the continuous loss of the dissolved active component which moreover needs to be separated from the effluent to avoid secondary contamination [3, 4]. Therefore, the CWPO processes of organic wastewater over heterogeneous catalysts using H_2O_2 as oxidant attracted much attention, and phenol was frequently chosen as a model pollutant in the studies, because it commonly exists in chemical industries [5]. Transition metal oxides and their complexes such as Fe [6], Cu [7] and Mn [8], other metals such as Al [9], Ce [10]and Au [11] were frequently used as active component for CWPO of phenol. The support materials of catalyst have been always considered as a key factor to influence the catalytic activity. And kinds of porous materials such as ZSM-5 [6], MCM-41 [12], SBA-15 [13], pillared clays [14], activated carbon [15] and graphite [16] were used as catalyst support for the CWPO of phenol aqueous solution.

The stability and deactivation of a heterogeneous catalyst has a significant impact on the oxidation of phenol wastewater and may seriously compromise the success of industrial application of CWPO technology. In this sense, a better understanding of deactivation mechanisms of the catalysts is needed, in order to properly design stable catalysts and instruct the regeneration strategies. Catalyst deactivation can occur by several mechanisms, such as sintering, poisoning of active sites, and metal leaching [17]. P. Bautista et al. [18] reported that the growth of Fe_2O_3 particle size and partial blockage of active site by deposition of carbon-containing matter on the catalyst surface could result in the deactivation of Fe-bearing catalysts. J.A. Zazo et al. [19] suggested that iron leaching and active sites blockage by polymeric deposits were the main causes resulted in the deactivation of Fe/active carbon catalyst. Most of the researches about CWPO processes of phenol and the deactivation studies of the catalysts were carried out in batch operations. However, there were many shortcomings existed in the batch reactor such as high concentration of complicated intermediate products and long contact time which resulted in the decrease of longevity of the

catalyst [20] and these drawbacks might be overcome by using a fixed bed reactor. Fernando Martínez et al. [21] reported a remarkable catalytic performance of iron oxide over different silica supports (meso-structured SBA-15 and non-ordered meso-porous silica), used for the CWPO of phenolic aqueous solution in a fixed bed reactor. They pointed out that the chemical alteration of the crystalline iron oxides could result in the partial deactivation of the catalyst. However, there is no literature systematically focused on the stability and deactivation study of heterogeneous catalyst over CWPO process of phenol in a fixed bed reactor, especially, in a membrane reactor.

In our previous work, novel Fe-ZSM-5 zeolite membrane catalysts were prepared for catalytic wet peroxide oxidation of phenol in a membrane reactor [22]. ZSM-5 zeolite membrane (about 6 μm) with a Si/Al ratio of 80 was successfully fabricated on the surface of PSSFs by a secondary growth method and the three dimension structure and unique surface properties of the ZSM-5 zeolite membrane made it to be an excellent support candidate. Fe element in a form of Fe_2O_3 was uniformly dispersed on the surface of ZSM-5 zeolite membrane support and the Fe-ZSM-5 zeolite membrane catalysts showed excellent catalytic activity when used for CWPO of phenolic aqueous solution in a membrane reactor. However, more meaningful work should be done to study the stability of the Fe-ZSM-5 zeolite membrane catalyst and the deactivation mechanisms of the catalyst should also be further investigated.

The aim of the present work is to (a) study the influence of residence time on the CWPO of phenol in the membrane reactor, (b) evaluate the stability of the Fe-ZSM-5 zeolite membrane catalyst at the best operation conditions, and (c) investigate the deactivation mechanisms of the catalyst.

2. Experimental

2.1 Material

Stainless steel fibers with average diameter of 6.5 μm were obtained from Huitong advanced material company (China). Tetrapropylammonium hydroxide (TPAOH, 25 wt.% aqueous) and cationic polymer (Poly(dimethylamine-co-epiclorohydrin), 50 wt.%) were obtained from Sigma-Aldrich. Ethanol (C_2H_5OH, >99.8%), sodium hydroxide (NaOH, 99%), sulfuric acid (H_2SO_4, 95-98%), ammonia water (NH_3, 25-28 wt.% aqueous) and sodium aluminate ($NaAlO_2$, Anhydrous) were all obtained from Sinopharm Chemical reagent Co., Ltd. Tetraethoxysilane (TEOS, >99%) and phenol were obtained from Guangzhou Chemical Reagent Factory. Hydrogen

peroxide (H_2O_2, 30 wt.% aqueous) was obtained from Jiangsu Qiangsheng Chemical Co., Ltd. Iron nitrate nonahydrate ($Fe(NO_3)_3•9H_2O$) was obtained from Tianjin Damao Chemical Reagent Factory. Manganese dioxide was obtained from Shanghai Qiangshun Chemical Reagent Factory. Sodium thiosulfate and potassium iodide were obtained from Tianjin Bodi chemical Co., Ltd. Deionized water was used in all synthesis process. All of the chemical reagents used in this study were analytical grade.

2.2 Preparation of Fe-ZSM-5 zeolite membrane catalyst

Details of the synthetic procedure of paper-like stainless sintered steel fibers (PSSFs) and ZSM-5 membrane/PSSFs were reported in our previous paper [23]. The preparation procedures of Fe-ZSM-5 zeolite membrane catalyst were concluded in Fig. 1. The Fe-ZSM-5 zeolite membrane was developed by the wet lay-up paper-making process, sintering process and secondary growth process. Firstly, stainless steel fibers (6.5 μm in diameter, 2-3 mm length) and cellulose with a mass ratio of 2:1 were added into 1 L water and stirred vigorously for 10 min to form a uniform suspension. A circular precursor paper was prepared by filtering the uniform suspension using a wet lay-up process, drying in air at 105 ℃ for 24 h, and then sintered in N_2 at 1050 ℃ for 30 min to destroy the cellulose and form a PSSFs support with three dimensional network structure. Secondly, synthesis of ZSM-5 zeolite membranes on the PSSFs support by secondary growth process. The silicalite-1 seeds were prepared by hydrothermal synthesis method using the synthesis solution with a molar ration 9TPAOH: 25TEOS: $500H_2O$: $100C_2H_5OH$. Then, the pretreated PSSFs support was dipped in a silicalite-1 seed solution (approximately 2 wt% aq.) to adsorb silicate-1 seeds on the surface and then air dried. The secondary synthesis solution with a molar composition 1 TEOS: 0.112 TPAOH: 0.0125 $NaAlO_2$: $111H_2O$ was prepared and the seeded PSSFs support was dipped vertically in a 200 mL Teflon lined autoclave at 150 ℃ for 48 hours. The synthesized samples were washed, air dried and calcined at 500 ℃ for 4 hours to remove the TPAOH. Finally, Fe active component was loaded on the ZSM-5 membrane by means of incipient wetness impregnation. Fe ions concentrations were adjusted to obtain 25 wt.% Fe loading on the catalyst. The sample was air dried at 100 ℃ for 12 h and calcined in air until 550 ℃ (6h) using a slow ramp of temperature (1 ℃/min).

2.3 Catalytic wet peroxide oxidation of phenol in a membrane reactor

Catalytic wet hydrogen peroxide oxidation experiments were carried out in a membrane

reactor made of a stainless steel tube (20 mm i.d., 100 mm length), operating at constant 80 ℃ of temperature under atmospheric pressure. The experimental set-up used for the oxidation of phenol aqueous solution by means of CWPO is showed in Fig. 2. The concentration of reactants in the feed tank was a mixture of phenol solution, 1000 mg/L of phenol and 5100 mg/L of H_2O_2 (stoichiometric amount for the total phenol oxidation according to reaction 1). The phenol aqueous solution was fed to the reactor in up-flow operation by a peristaltic pump. The membrane reactor was heated by a thermal bath.

$$C_6H_5OH + 14H_2O_2 \rightarrow 6CO_2 + 17H_2O \qquad (1)$$

Samples were hourly withdrawn from the treated effluent and diluted 10 times. H_2O_2 concentration was firstly determined by iodometric titration using a 0.02 mol/L sodium thiosulfate solution. For the purpose of eliminating residual H_2O_2 from the diluted samples, all the diluted solutions were mixed with 0.1 g manganese dioxide at least 15 min before measuring the phenol concentration, total organic carbon (TOC) concentration, and iron leaching concentration. Phenol concentration was measured by an HPLC Chromatograph (Agilent 1100) equipped with a Agilent HC-C18(2) column and a UV detector adjusted at 210 nm. The methanol and ultrapure water (v/v= 40:60) was chosen as the mobile phase. TOC concentration of the samples was measured by a Liqui TOC (Elementar, Germany). Iron leaching concentration in the treated effluent was tested by an atomic absorption spectrophotometer (AA240FS, Varian Co., USA). The H_2O_2 conversion (X_{H2O2}, %), the phenol conversion (X_{phenol}, %) and TOC conversion (X_{TOC}, %) are defined as follows:

$$X_{H_2O_2} = \frac{C_{H_2O_2(in)} - C_{H_2O_2(out)}}{C_{H_2O_2(in)}} \times 100\% \qquad (2)$$

$$X_{phenol} = \frac{C_{phenol(in)} - C_{phenol(out)}}{C_{phenol(in)}} \times 100\% \qquad (3)$$

$$X_{TOC} = \frac{C_{TOC(in)} - C_{TOC(out)}}{C_{TOC(in)}} \times 100\% \qquad (4)$$

Where $C_{H2O2(in)}$ (mg/L) and $C_{H2O2(out)}$ (mg/L) are the concentrations of H_2O_2 in the inlet and outlet of the solution, respectively, $C_{phenol(in)}$ (mg/L) and $C_{phenol(out)}$ (mg/L) are the concentrations of phenol in the inlet and outlet solution, respectively, and $C_{TOC(in)}$ (mg/L) and $C_{TOC(out)}$ (mg/L) are

the concentrations of TOC in the inlet and outlet solution, respectively.

2.4 Stability of the Fe-ZSM-5 zeolite membrane catalyst

The long-term activity of Fe-ZSM-5 zeolite membrane catalyst was tested for the treatment of phenol aqueous solution. The catalyst was used continuously up to 40 hours at the catalyst bed height of 4.0 cm, the flow speed rate of 2 mL/min and the temperature of 80 ℃. Meanwhile, the conversions of phenol, hydrogen peroxide and TOC as well as iron leaching concentration in the solution were monitored.

2.5 Deactivate mechanism of the Fe-ZSM-5 zeolite membrane catalyst

The crystallographic structures of the fresh and used Fe-ZSM-5 zeolite membrane catalyst samples were studied by X-ray diffraction patterns carried out on a PANalytical X'Pert Pro X-ray diffractometer using Cu Kα radiation, with a fixed power source (40 kV, 40 mA) and 2θ range from 5 to 90°. The textural and morphological information of the samples were characterized using field emission scanning electronic microscopy on a Zeiss Merlin FE-SEM. N_2 adsorption-desorption isotherms of catalyst samples were tested using a Micromeritics Tristar Ⅱ Surface Area and Porosity (Micromeritics Instrument Co., USA) at 77K. The sample was out-gassed on a Micromeritics Vacrep O61 Sample Degas System at 523K for 6 hours before measurement. Thermal gravimetric analysis of the fresh and used Fe-ZSM-5 zeolite membrane catalysts were investigated using thermo gravimetric analysis in nitrogen on a SDT Q600 (TA instrument Co., USA). Nitrogen flow rate was 100mL/min with a heating rate of 10 ℃/min, from room temperature to 800 ℃. Fourier transform infrared spectra of the fresh and used Fe-ZSM-5 zeolite membrane catalysts were obtained from a Perkin-Elmer Spectroscopy 100 with a resolution of 4 cm^{-1} in the range from 400 to 4000 cm^{-1} at room temperature. A typical pellet containing 1 wt.% of sample was prepared by mixing 1 mg sample with 100 mg KBr. Raman spectra were recorded on a Lab RAM Aramis Raman Spectrometer (HORIBA JOBIN YVON, France) with the spectrum range from 200 to 1600 cm^{-1}, using 632.81 nm laser as the spectrum source.

3. Results and discussion

3.1 Effects of residence time on the CWPO of phenol in a membrane reactor

The residence time of flowing material in the fixed bed reactor is defined in reference [24]. The catalytic volume (catalyst bed height) or volumetric flow rate (feed flow rate) can be adjusted to

study the influence of residence time on the CWPO of phenol in the fixed bed reactor.

In this research, the influence of the residence time on the CWPO of phenol in the fixed bed reactor was studied by modifying the catalyst bed height for 2.0 cm, 3.0 cm, and 4.0 cm while other operation parameters were kept as constants (namely, the feed flow rate of 2.0 mL/min, and the temperature of 80 ℃). The conversions of phenol, H_2O_2 and TOC, as well as the Fe leaching concentrations in the treated effluent were measured.

The experimental results are shown in Fig. 3. As can be seen in Fig. 3(a), phenol conversion increased with the catalyst bed height increased. Phenol conversion of 100% was obtained when the catalyst bed height reached 4.0 cm. Meanwhile, H_2O_2 conversion depicted in Fig. 3(b) kept the same variation trend as phenol conversion, increased obviously with the catalyst bed height increased. The H_2O_2 conversion reached above 99.0% and kept steady trend when phenol conversion reached 100% at the catalyst bed height of 4.0 cm. However, the H_2O_2 conversion decreased to 80.0% and 60.0%, but the phenol conversion still kept high conversion above 92.0% when the catalyst bed height decreased to 3 cm and 2 cm. These results showed that the catalytic reaction was not according to the stoichiometric amount for the total phenol oxidation. The phenol was partially oxidized and generated some intermediate products and low-molecular-weight organic acids [25]. The residual TOC was contributed to these low-molecular-weight organic acids (which were more resistant to oxidation) evolved by the primary products from phenol ring opening and continue oxidation of aromatics intermediates [20]. As can be seen in Fig. 3(c), TOC conversion increased from 40.0% to 60.0% when the catalyst bed height increased from 2 cm to 4 cm. Phenol conversion of 100% and H_2O_2 conversion about 99.0% did not attribute to the 100% TOC conversion because the H_2O_2 was partly decomposed into oxygen which was not capable to oxidize phenol under mild condition and generated some carboxylic acids such as formic, acetic and oxalic acids which were detected by HPLC analysis as shown in Fig. S2. All of above showed that the higher the catalyst bed height, which leaded to longer residence time, so the higher phenol conversion, H_2O_2 conversion and TOC conversion can be obtained.

The Fe leaching concentration in the treated effluent was hourly recorded and the results are showed in Fig. 3(d). The Fe leaching concentration increased with the catalyst bed height increased: about 5 mg/L, 15mg/L and 50mg/L at the catalyst bed height of 2 cm, 3 cm and 4 cm, respectively. This is due to the use of higher catalyst bed height (longer residence time) could

produce a higher loss of Fe ions in the liquid solution. Similar results were found by Fernando Martínez using Fe_2O_3/SBA-15 as catalyst in CWPO of phenolic effluents [21].

3.2 Stability of the Fe-ZSM-5 zeolite membrane catalyst

The long-term experiment of CWPO of phenol aqueous solution over the Fe-ZSM-5 zeolite membrane catalyst was carried out in a membrane reactor in order to test the stability of the catalyst. The catalyst was used in continuous operation up to 40 hours at the catalyst bed height of 4.0 cm, the flow speed rate of 2 mL/min and the temperature of 80 ℃. Meanwhile, the conversions of phenol, hydrogen peroxide and TOC as well as iron leaching concentration in the treated effluent were monitored and the results were depicted in Fig. 4. It can be found in Fig. 4(a), (b) and (c), phenol conversion decreased from 100% to 85%, H_2O_2 conversion decreased from 99.0% to 65.0%, and TOC conversion decreased from 60.0% to 49.0% after used 40 hours, respectively. As can be seen in Fig. 4(d), iron leaching concentration in the treated effluent showed a maximum concentration (about 50 mg/L) between 1 and 8 hour, and the concentration decreased to 0.5 mg/L after used 40 hours. These results showed that good stability of the Fe-ZSM-5 zeolite membrane catalyst was observed although the activity of the catalyst decreased after used 40 hours.

3.3 Deactivation study of Fe-ZSM-5 zeolite membrane catalyst

To study the deactivate mechanism of Fe-ZSM-5 zeolite membrane catalyst, the fresh and used catalyst was characterized by N_2 adsorption-desorption, XRD, FE-SEM, TGA, FT-IR and Raman spectra.

3.3.1 N_2 adsorption-desorption isotherms

Specific surface areas and porosity properties of fresh and used Fe-ZSM-5 zeolite membrane catalysts were characterized by N_2 adsorption-desorption. The N_2 adsorption-desorption isotherms of the catalysts were displayed in Fig. 5, and the BET surface areas and pore properties were summarized in Table 1. The specific surface areas (S_{BET}) were calculated from adsorption branches in the relative pressure range of 0.06-0.3 using the Brunauer-Emmett-Teller method. The total pore volume (V_t) was estimated by analysis the N_2 adsorption-desorption isotherms, the micropore volume (V_{micro}) and mesopore volume (V_{meso}) were calculated using the t-plot method and the Barrett-Joyner-Halenda (BJH) method, respectively. Fig. 5 shows that the volume adsorbed increases with increasing relative pressures for all isotherms which is due to the volume filling of

micropores in ZSM-5 zeolite membrane. The volume adsorbed increases continually when the relative pressures increase, which should be caused by the multilayer adsorption. Both of the catalysts show a similar hysteresis loop at a high relative pressure fit for type IV of adsorption isotherms which are given by many mesoporous adsorbents [26]. The hysteresis loop is associated with capillary condensation taking place in mesopores, and the limiting uptake over a range of high relative pressure. As listed in Table 1, the BET specific surface area and total pore volume of used Fe-ZSM-5 zeolite membrane catalyst were 126.0 m^2/g and 0.09481 cm^3/g, respectively. The fresh Fe-ZSM-5 zeolite membrane catalyst exhibited higher BET specific surface area (177.4 m^2/g) and total pore volume (0.1280 cm^3/g) than the used one. Meanwhile, the volumes of total pores and micropores decreased from 0.1280 cm^3/g to 0.09481 cm^3/g and from 0.05651 cm^3/g to 0.03872 cm^3/g, respectively. The decreases of volume may result from the blockage of the Fe-ZSM-5 zeolite membrane catalyst. It can be concluded that the decreases of BET surface area and volume blockage have resulted in the deactivation of the Fe-ZSM-5 zeolite membrane catalyst. These results indicated that the surface characteristics and pore structures of Fe-ZSM-5 zeolite membrane catalyst were changed after continuously using 40 hours.

Table 1. Physiochemical properties of the catalysts.

Sample	S_{BET} (m^2/g)	V_t (cm^3/g)	V_{micro} (cm^3/g)	V_{meso} (cm^3/g)
Fresh Fe-ZSM-5[a]	177.4	0.1280	0.05651	0.06309
Used Fe-ZSM-5[b]	126.0	0.09481	0.03872	0.05556

a Relative to fresh Fe-ZSM-5 zeolite membrane catalyst.
b Relative to used Fe-ZSM-5 zeolite membrane catalyst.

3.3.2 X-ray diffraction (XRD) analysis

The crystallographic structures of the fresh Fe-ZSM-5 zeolite membrane catalyst and used Fe-ZSM-5 zeolite membrane catalyst (8 hours) and (40 hours) were studied by X-ray diffraction patterns, as shown in Fig. 6. All of the XRD patterns showed the diffraction peaks at the ranges of 2θ=7-9° and 2θ=23-25°, matching well with the standard phase of ZSM-5 zeolite [27], indicating that the ZSM-5 zeolite was still well crystallized after using 40 hours. Two peaks of iron oxide at 2θ=33.0° and 2θ=35.6° were detected but its peaks intensity decreased compared with the fresh catalyst. This could be attributed to the loss of Fe_2O_3 component which distributed out of the zeolite membrane surface. It can be seen from Fig. 6(b) that no other changes happened but the peak intensities of the used catalyst decreased which indicated the loss of Fe species after used 8

hours and this is in agreement with the Fe leaching concentration depicted in Fig. 4(d). Meanwhile, two new peaks of carbon around 45° and 75° were observed in the Fe-ZSM-5 zeolite membrane catalyst after used 40 hours, as shown in Fig. 6(c). The existence of carbon may lead to a partial blockage of active sites. P. Bautista et al. [18] concluded that the presence of carbon-containing matter adsorbed onto the catalyst had a negative effect on the catalytic activity.

3.3.3 Field emission scanning electron microscopy analysis

Morphology and structure of the fresh and used Fe-ZSM-5 zeolite catalysts were investigated by FE-SEM. Fig. 7 shows the FE-SEM images of fresh and used Fe-ZSM-5 zeolite membrane catalysts. Fig. 7(a) and (c) clearly show that the junctures of stainless steel fibers were sintered together to form a three dimention network structure and Fe_2O_3 active component was uniformly destributed on the surface of ZSM-5 zeolite membrane. Microstructure and morphological information of the used Fe-ZSM-5 zeolite membrane catalyst are shown in Fig. 7(b) and (d) respectively. As can be seen in Fig. 7(b), the space of ZSM-5 zeolite membrane was blocked and thus resulted in the loss of three dimension structure of PSSFs. Morphological information of the used Fe-ZSM-5 zeolite membrane catalyst shows that the active Fe_2O_3 component could not uniformly disperse on the surfaces of ZSM-5 zeolite membrane. As can be seen in Fig. 7(d), some cracks are detected on the zeolite membrane, and this could influence the activity of the catalyst. The XRD pattern with low peaks intensity discussed before can be explained.

3.3.4 Thermal gravimetric analysis

TGA and DTA experiments of the used and fresh Fe-ZSM-5 zeolite membrane catalysts were conducted, and the results were shown in Fig. 8 and Fig. 9. As can be seen in Fig. 8(a), slight weight loss (about 2%) below 110 ℃ was observed, which could be assigned to the evaporation of adsorbed molecular water, and no weight loss occurred from 110 to 800 ℃. Meanwhile, two weight losses (about 1% and 3%) were observed from 110 to 800 ℃ in the used catalyst shown in Fig. 8(b). Fig. 9(a) and (b) showed the DTA curves of the fresh and used catalyst, respectively. Two new exothermic peaks at 186 ℃ and 376 ℃ were observed in Fig. 9(b). Caerio et al. [28] observed that the presence of two types of coke molecular which denoted as “light coke” (monoaromatic polysubstituted compounds) and “hard coke” (polyaromatic compounds). Hosseini et al. [29] observed two exothermic peaks at 325 ℃ and 525 ℃ which they related to the light and hard coke, respectively. Meanwhile, two peaks at 202 ℃ and 286 ℃ were observed by T. Barakat

et al. [30], and they concluded that the first peak was attributed to the removal of lightly adsorbed aromatic molecules and the second peak was attributed to the removal of highly adsorbed aromatic molecules formed by the degradation of toluene. So, the two peaks of the used Fe-ZSM-5 zeolite membrane catalyst could be attributed to the removal of light coke (phenol etc.) and hard coke (polyaromatic compounds). The deposition of carbonaceous compounds on the active sites could result in the deactivation of Fe-ZSM-5 zeolite membrane catalyst, and this could also be verified by XRD and SEM analysis.

3.3.5 Fourier transform infrared spectra analysis

FT-IR spectra of the fresh and used Fe-ZSM-5 zeolite membrane catalyst showed all the bands characterizing skeletal vibrations of MFI zeolite structure. As can be seen in Fig. 10, The band around 543 cm^{-1} was typically due to the pentasil framework variation and the ratio of band intensities at 550 and 450 cm^{-1} was often used as an indication of zeolite crystallinity [31]. The absorption band around 796 cm^{-1} was due to Si-O-Si symmetric stretching, and absorption band around 1099 and 1230 cm^{-1} were assigned to asymmetric stretching of Si-O-Si [32]. The weak absorption band around 3499 cm^{-1} implies the existence of hydroxyl groups [33]. The relative intensity of used Fe-ZSM-5 zeolite membrane catalyst decreased and two new weak absorption bands around 1359 and 1315 cm^{-1} were observed in the catalyst used for 40 hours. The absorption bands around 1300-1700 cm^{-1} (bands of C-H deformation and C-C stretching vibration) were investigated by G. Caeiro et al [28] and they concluded that the integrated surface in the 1300-1700 cm^{-1} region is proportional to the amount of carbon in the zeolite. So, the newly observed absorption bands around 1359 and 1315 cm^{-1} could be due to the carbon coked on the surface of the catalyst. FT-IR patterns of the catalyst after used 8 hours showed that no absorption band around 1359 cm-1 was observed and this indicated that no carbon deposition happened in the first 8 hours, and this is in agreement with the XRD results discussed before. It can be concluded that the initial deactivation of the catalyst is caused by the leaching of Fe and the deactivation occurred later is partly caused by carbon deposition. The decreased intensity of used catalyst revealed that the crystalline property of the ZSM-5 membrane was changed.

3.3.6 Raman spectra analysis

To investigate the surface information of the used and fresh Fe-ZSM-5 zeolite membrane catalysts, Raman spectra were performed and the results were depicted in Fig. 11. As can be seen

in Fig. 11, Raman shift bands around 220, 286, 398, 602 and 652 cm^{-1} were observed on the used and fresh Fe-ZSM-5 zeolite membrane catalysts. Meanwhile, additional bands at 132, 162 and 490 cm^{-1} were observed on the used catalyst. The bands around 220, 286, 398, 602 and 652 cm^{-1} were assigned to the standard Raman spectrum of hematite (α-Fe_2O_3) [34, 35]. D.Bersani et al. [36]investigated the Raman spectra of common iron oxide with different phase, namely, hematite (α-Fe_2O_3), maghemite (γ-Fe_2O_3), magnetite (Fe_3O_4) and goethite (α-FeOOH). They found that the existence of maghemite would make the Raman spectrum of hematite complex. So, the additional bands on the used catalyst could result from the co-existence of the two phases (α-Fe_2O_3 and γ-Fe_2O_3). It can be concluded from the Raman spectra that part of the active component changed fromα-Fe_2O_3 phase to γ-Fe_2O_3 phase after used 40 hours. This was another reason that resulted in the deactivation of the Fe-ZSM-5 zeolite membrane catalyst.

4. Conclusions

In conclusion, a novel Fe-ZSM-5 zeolite membrane catalyst was prepared for catalytic wet peroxide oxidation of phenol in a membrane reactor. Longer residence time had a positive effect on the CWPO of phenol over the Fe-ZSM-5 zeolite membrane catalyst. The complete phenol conversion, high TOC conversion about 60.0% and the H_2O_2 conversion above 99.0% were achieved at the optimized condition, namely, at the catalyst bed height of 4.0 cm (the longest residence time), the temperature of 80 ℃, and H_2O_2 concentration of 5100 mg/L, respectively. Meanwhile, good stability with low Fe leaching concentration (about 0.5 mg/L) and high phenol conversion (above 85%) were obtained after successive ran for 40 hours. Furthermore, the loss of active component in the first 8 hours, partial phase change from α-Fe_2O_3 to γ-Fe_2O_3, the crystalline change of the ZSM-5 zeolite membrane support and the coke formations on the surface of the catalyst were found to be responsible for the deactivation of the catalysts. Further research should focus on the regeneration strategies of the Fe-ZSM-5 zeolite membrane catalyst.

Supplementary Material

TGA profiles of the uncalcined Fe-ZSM-5 zeolite membrane catalyst (Fig. S1); HPLC pattern of reaction by-products after CWPO of phenol, (peak 1: phenol; peak 2: acetic acid; peak 3: formic acid; peak 4: oxalic acid), (Fig. S2); the standard XRD patterns of α-Fe2O3 and γ-Fe2O3 from JCPDS files (Fig. S3).

Acknowledgement

We gratefully acknowledge the financial support of the National Natural Science Foundation of China (Grant No. 21176086 and 21376101).

References:

1. A. D. Bokare and W. Choi, *Journal of Hazardous Materials*, 2014, 275, 121-135.
2. G. Busca, S. Berardinelli, C. Resini and L. Arrighi, *Journal of Hazardous Materials*, 2008, 160, 265-288.
3. E. G. Garrido-Ramírez, B. K. G. Theng and M. L. Mora, *Applied Clay Science*, 2010, 47, 182-192.
4. L. F. Liotta, M. Gruttadauria, G. Di Carlo, G. Perrini and V. Librando, *Journal of Hazardous Materials*, 2009, 162, 588-606.
5. V. S. Mishra, V. V. Mahajani and J. B. Joshi, *Industrial & Engineering Chemistry Research*, 1995, 34, 2-48.
6. K. Fajerwerg and H. Debellefontaine, *Applied Catalysis B: Environmental*, 1996, 10, L229-L235.
7. N. Inchaurrondo, J. Cechini, J. Font and P. Haure, *Applied Catalysis B: Environmental*, 2012, 111-112, 641-648.
8. E. Saputra, S. Muhammad, H. Sun, H. Ang, M. O. Tadé and S. Wang, *Applied Catalysis B: Environmental*, 2013, 142-143, 729-735.
9. J. Barrault, M. Abdellaoui, C. Bouchoule, A. Majesté, J. M. Tatibouët, A. Louloudi, N. Papayannakos and N. H. Gangas, *Applied Catalysis B: Environmental*, 2000, 27, L225-L230.
10. P. Massa, F. Ivorra, P. Haure and R. Fenoglio, *Journal of Hazardous Materials*, 2011, 190, 1068-1073.
11. A. Quintanilla, S. García-Rodríguez, C. M. Domínguez, S. Blasco, J. A. Casas and J. J. Rodriguez, *Applied Catalysis B: Environmental*, 2012, 111-112, 81-89.
12. S. Chaliha and K. G. Bhattacharyya, *Chemical Engineering Journal*, 2008, 139, 575-588.
13. X. Zhong, J. Barbier Jr., D. Duprez, H. Zhang and S. Royer, *Applied Catalysis B: Environmental*, 2012, 121-122, 123-134.
14. E. Guélou, J. Barrault, J. Fournier and J. Tatibouët, *Applied Catalysis B: Environmental*, 2003, 44, 1-8.
15. S. A. Messele, O. S. G. P. Soares, J. J. M. Órfão, F. Stüber, C. Bengoa, A. Fortuny, A. Fabregat and J. Font, *Applied Catalysis B: Environmental*, 2014, 154-155, 329-338.
16. C. M. Domínguez, P. Ocón, A. Quintanilla, J. A. Casas and J. J. Rodriguez, *Applied Catalysis B: Environmental*, 2014, 144, 599-606.
17. S. K. Bhargava, J. Tardio, J. Prasad, K. Föger, D. B. Akolekar and S. C. Grocott, *Industrial & Engineering Chemistry Research*, 2006, 45, 1221-1258.
18. P. Bautista, A. F. Mohedano, N. Menéndez, J. A. Casas and J. J. Rodriguez, *Catalysis Today*, 2010, 151, 148-152.
19. J. A. Zazo, J. A. Casas, A. F. Mohedano and J. J. Rodríguez, *Applied Catalysis B: Environmental*, 2006, 65, 261-268.
20. G. Centi, S. Perathoner, T. Torre and M. G. Verduna, *Catalysis Today*, 2000, 55, 61-69.
21. F. Martínez, J. A. Melero, J. Á. Botas, M. I. Pariente and R. Molina, *Industrial & engineering chemistry research*, 2007, 46, 4396-4405.
22. Y. Yan, S. Jiang, H. Zhang and X. Zhang, *Chemical Engineering Journal*, 2015, 259,

243-251.
23. H. Chen, H. Zhang and Y. Yan, *Chemical Engineering Journal*, 2012, 209, 372-378.
24. O. Levenspiel, *Chemical Reaction Engineering*. Wiley New York etc.: 1972; Vol. 2.
25. J. A. Zazo, J. A. Casas, A. F. Mohedano and J. J. Rodríguez, *Applied Catalysis B: Environmental*, 2006, 65, 261-268.
26. K. S. W. Sing, D. H. Everett, R. A. W. Haul, L. Moscou, R. A. Pierotti, J. Rouquérol and T. Siemieniewska, *Pure Applied Chemistry*, 1985, 57, 603-619.
27. M. M. Treacy, J. B. Higgins, R. von Ballmoos, I. Z. Association and S. Commission, *Collection of simulated XRD powder patterns for zeolites*. Elsevier New York: 1996; Vol. 552.
28. G. Caeiro, J. M. Lopes, P. Magnoux, P. Ayrault and F. Ramôa Ribeiro, *Journal of Catalysis*, 2007, 249, 234-243.
29. M. Hosseini, S. Siffert, H. L. Tidahy, R. Cousin, J. F. Lamonier, A. Aboukais, A. Vantomme, M. Roussel and B. L. Su, *Catalysis Today*, 2007, 122, 391-396.
30. T. Barakat, V. Idakiev, R. Cousin, G. S. Shao, Z. Y. Yuan, T. Tabakova and S. Siffert, *Applied Catalysis B: Environmental*, 2014, 146, 138-146.
31. N. H. Phu, T. T. K. Hoa, N. V. Tan, H. V. Thang and P. L. Ha, *Applied Catalysis B: Environmental*, 2001, 34, 267-275.
32. Y. Meng, H. C. Genuino, C. Kuo, H. Huang, S. Chen, L. Zhang, A. Rossi and S. L. Suib, *Journal of the American Chemical Society*, 2013, 135, 8594-8605.
33. Y. Wang, H. Sun, H. M. Ang, M. O. Tadé and S. Wang, *Chemical Engineering Journal*, 2014, 245, 1-9.
34. C. di Luca, F. Ivorra, P. Massa and R. Fenoglio, *Industrial & Engineering Chemistry Research*, 2012, 51, 8979-8984.
35. D. L. A. de Faria, S. Venâncio Silva and M. T. de Oliveira, *Journal of Raman Spectroscopy*, 1997, 28, 873-878.
36. D. Bersani, P. P. Lottici and A. Montenero, *Journal of Raman Spectroscopy*, 1999, 30, 355-360.

Figure contents:

Fig. 1. Preparation procedure of Fe-ZSM-5 zeolite membrane catalyst.

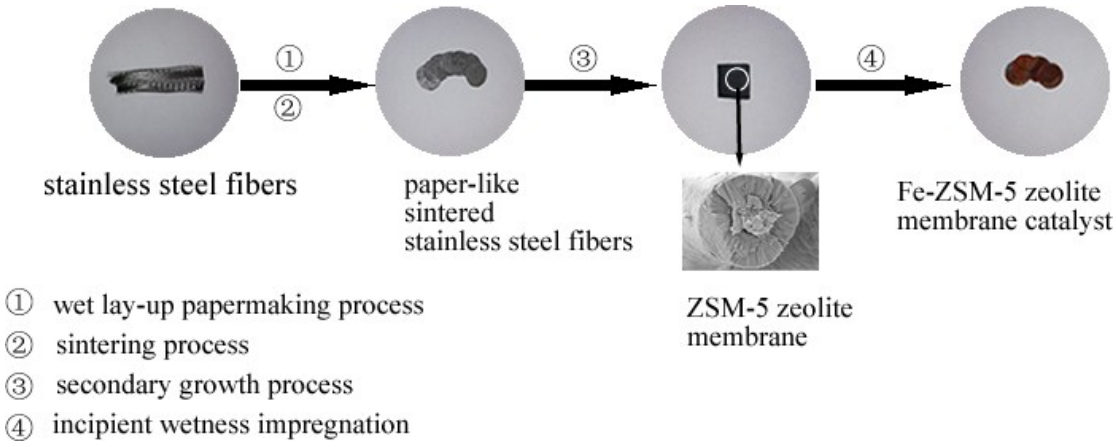

① wet lay-up papermaking process
② sintering process
③ secondary growth process
④ incipient wetness impregnation

Fig. 2. Flowchart of the experimental set-up.

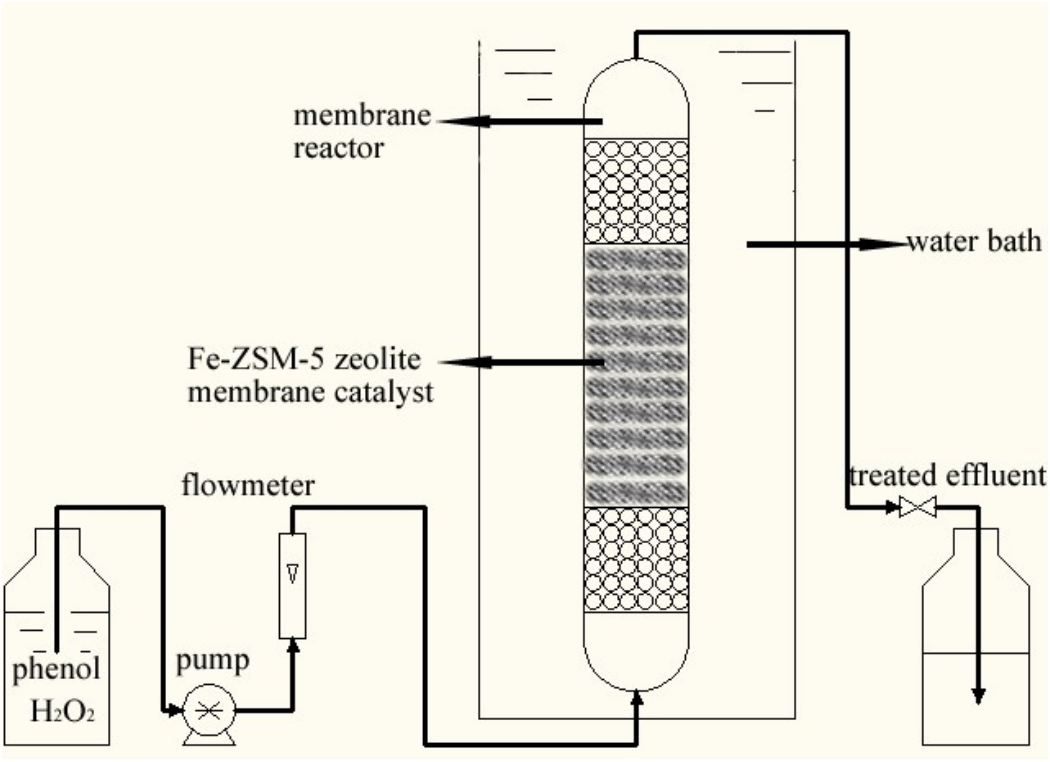

Fig. 3. Effects of the catalyst bed height (residence time)on the catalytic performance: (a) phenol conversion (X_{phenol}), (b) H_2O_2 conversion (X_{H2O2}), (c) TOC conversion (X_{TOC}), and (d) Fe leaching concentration (C_{Fe}), respectively.

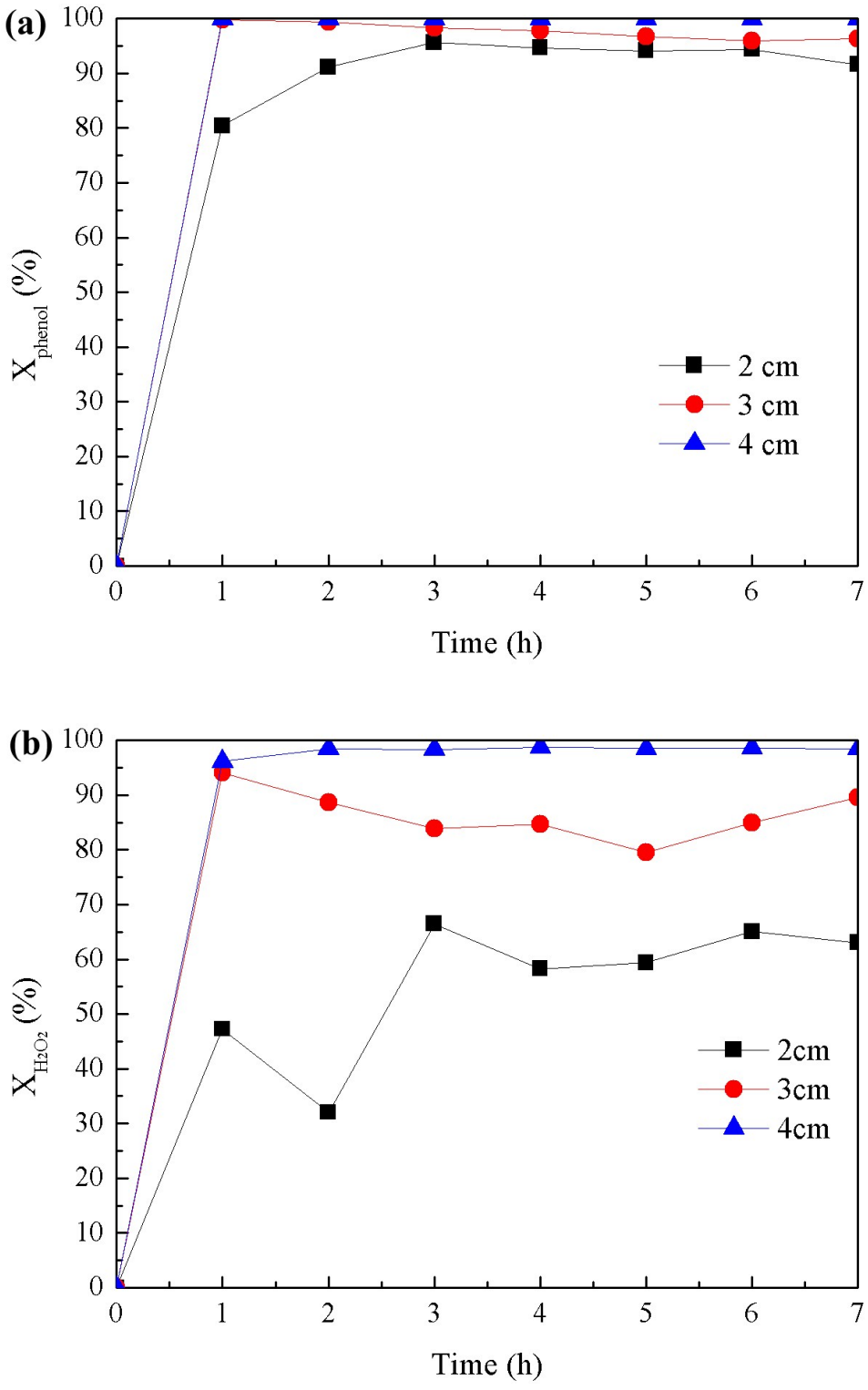

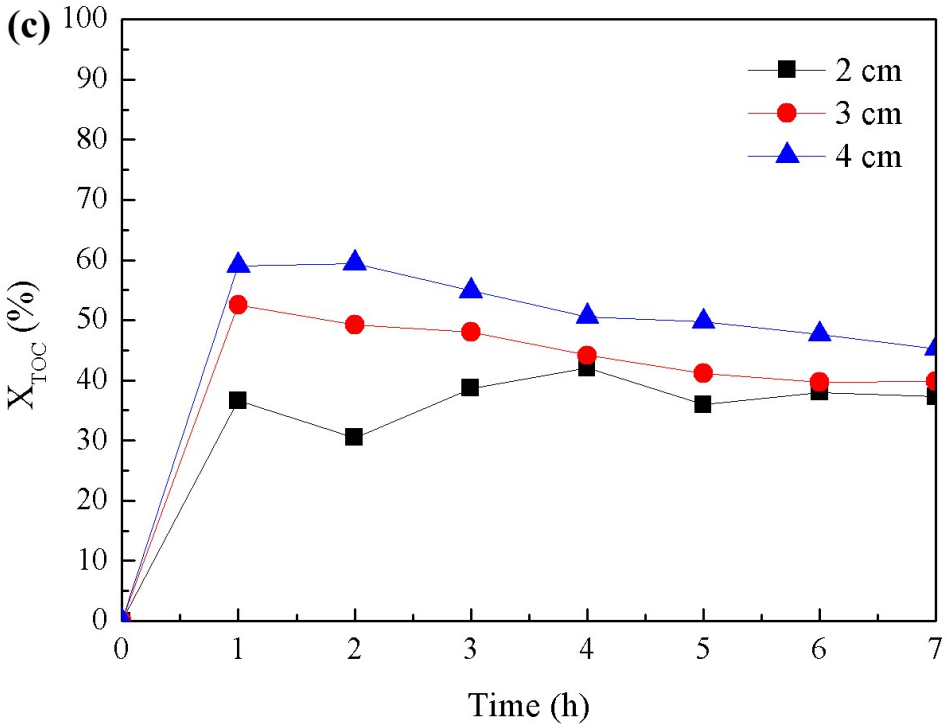

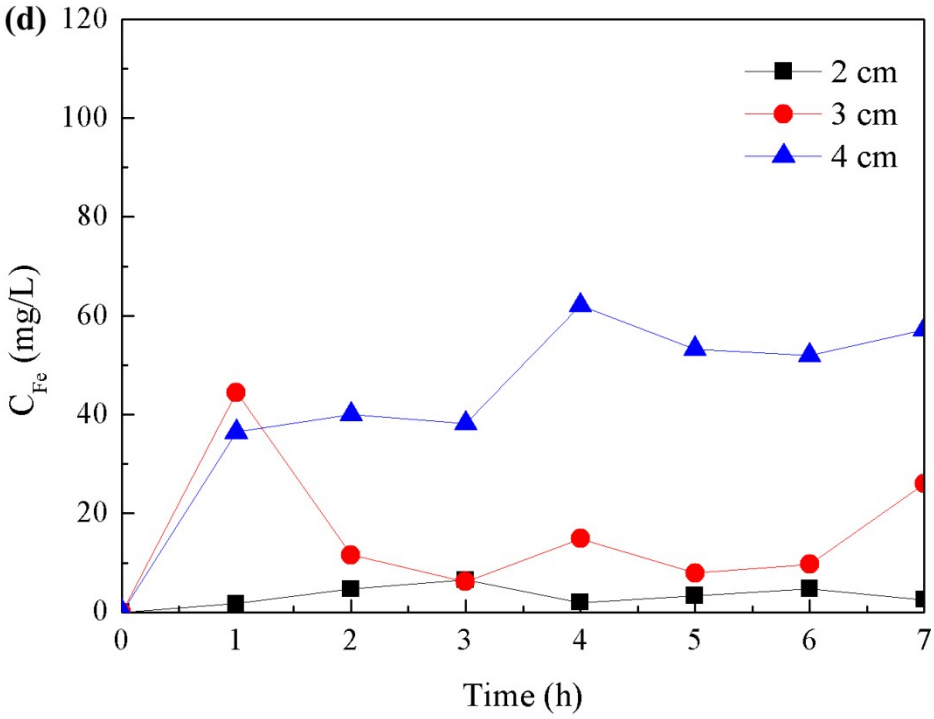

Fig. 4. Stability of the Fe-ZSM-5 zeolite membrane catalyst: (a) phenol conversion (X_{phenol}), (b) H_2O_2 conversion (X_{H2O2}), (c) TOC conversion (X_{TOC}), and (d) Fe leaching concentration (C_{Fe}), respectively.

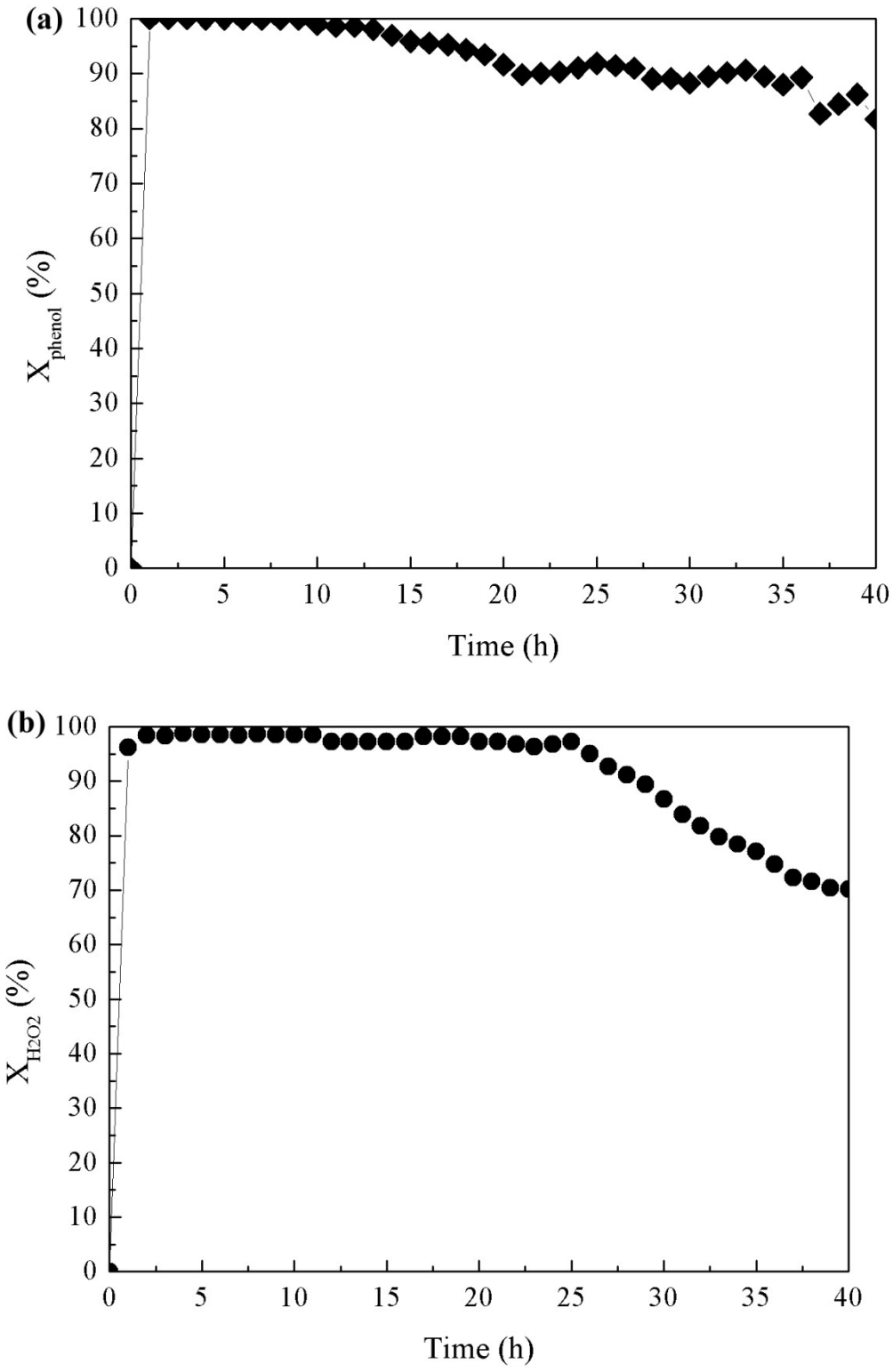

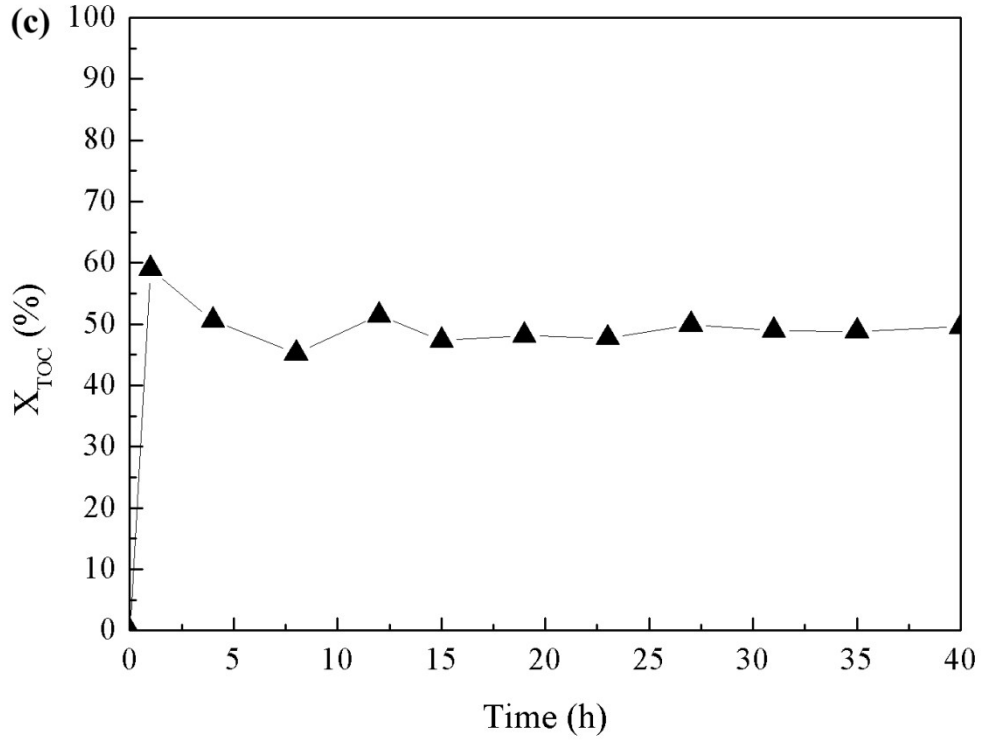

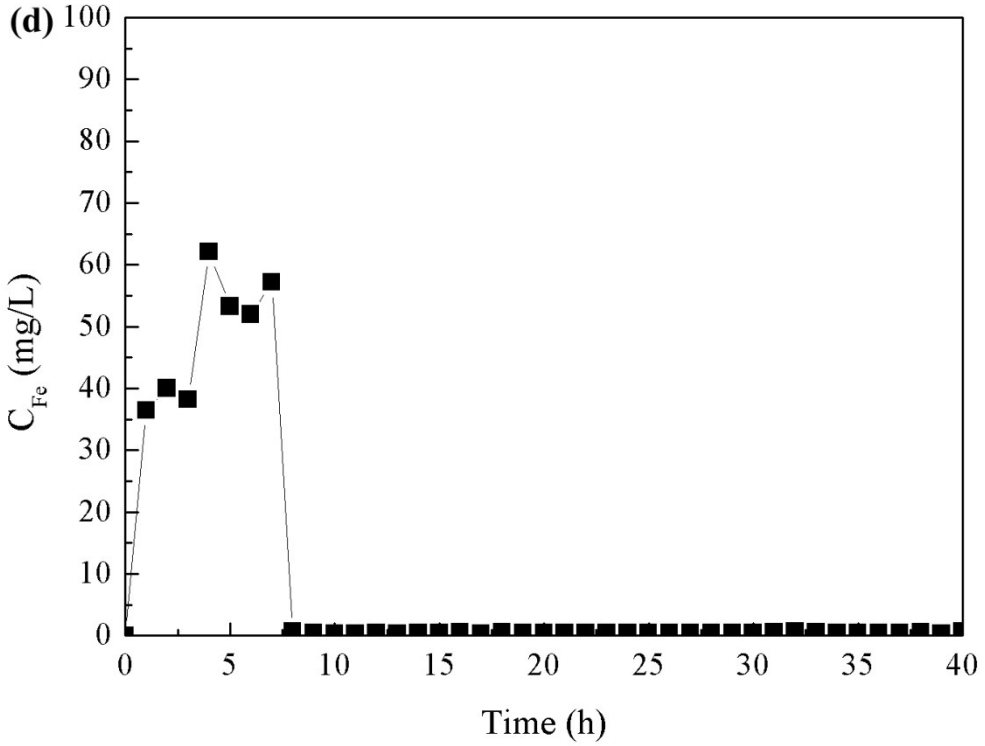

Fig. 5. N_2 adsorption-desorption isotherms of the catalysts at 77 K: (a) fresh Fe-ZSM-5 zeolite membrane catalyst, and (b) used Fe-ZSM-5 zeolite membrane catalyst, respectively.

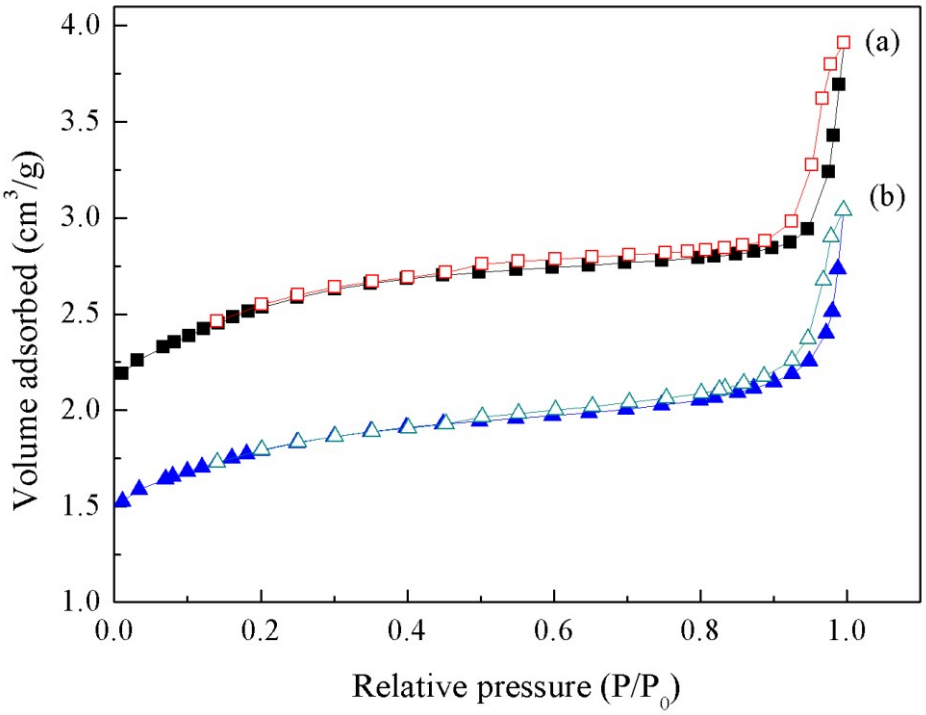

Fig. 6. XRD patterns of the samples: (a) fresh Fe-ZSM-5 zeolite membrane catalyst (b) used Fe-ZSM-5 zeolite membrane catalyst (8 hours) and (c) used Fe-ZSM-5 zeolite membrane catalyst (40 hours), respectively.

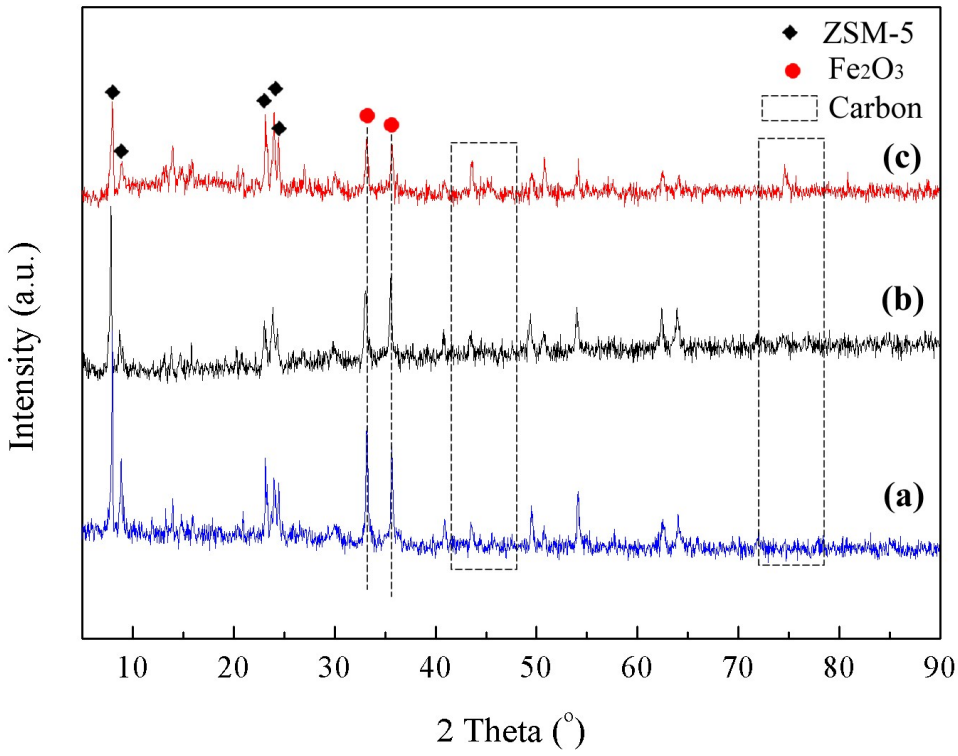

Fig. 7. FE-SEM images of the catalyst samples: (a) fresh Fe-ZSM-5 zeolite membrane catalyst, (b) used Fe-ZSM-5 zeolite membrane catalyst, (c) morphological information of the fresh Fe-ZSM-5 zeolite membrane catalyst, and (d) cross-sectional SEM image of the used Fe-ZSM-5 zeolite membrane catalyst, respectively.

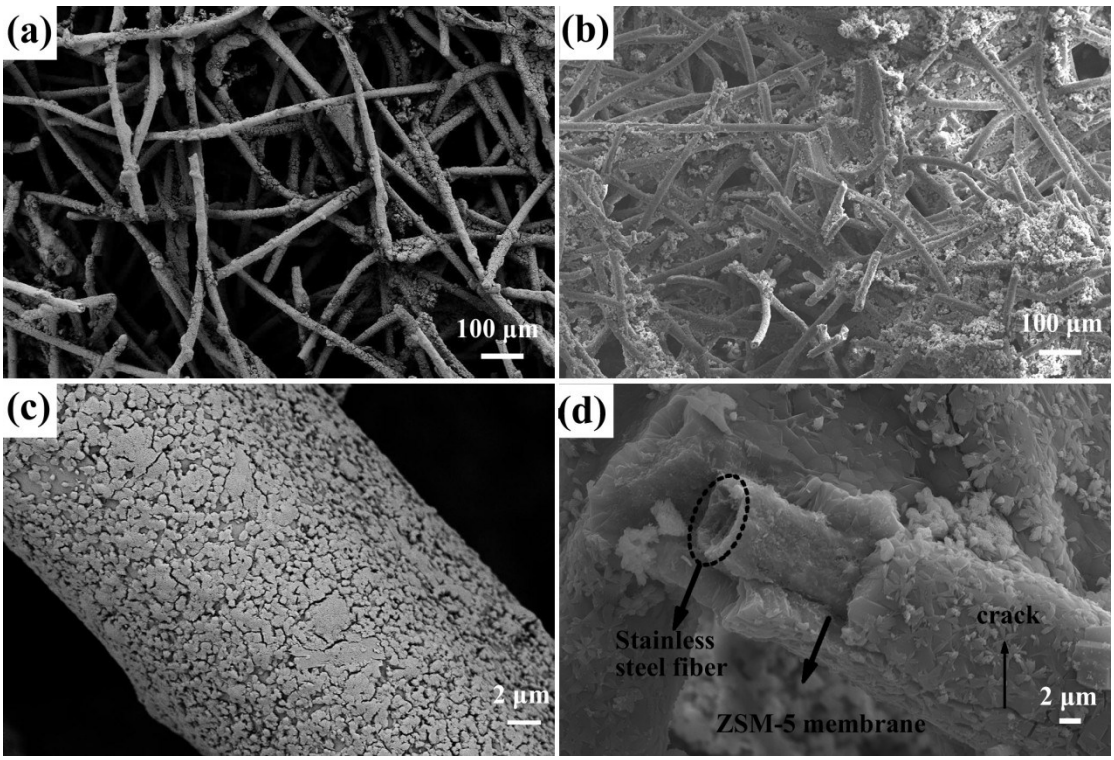

Fig. 8. TGA profiles of the catalyst samples: (a) fresh Fe-ZSM-5 zeolite membrane catalyst, and (b) used Fe-ZSM-5 zeolite membrane catalyst, respectively.

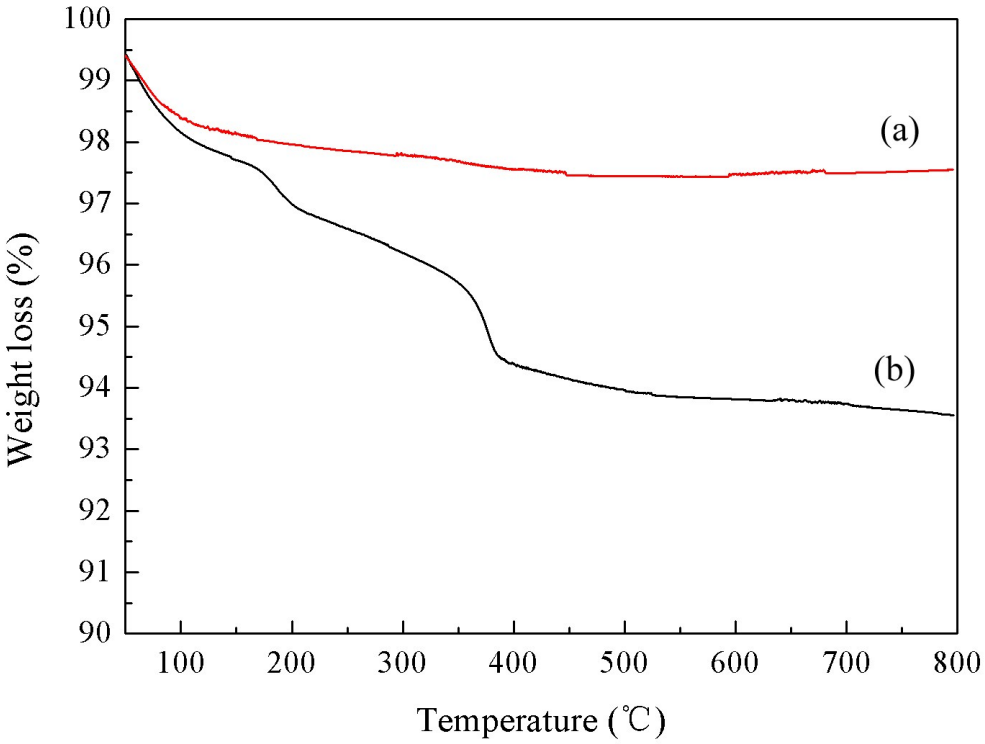

Fig. 9. DTA profiles of the catalyst samples: (a) fresh Fe-ZSM-5 zeolite membrane catalyst, and (b) used Fe-ZSM-5 zeolite membrane catalyst, respectively.

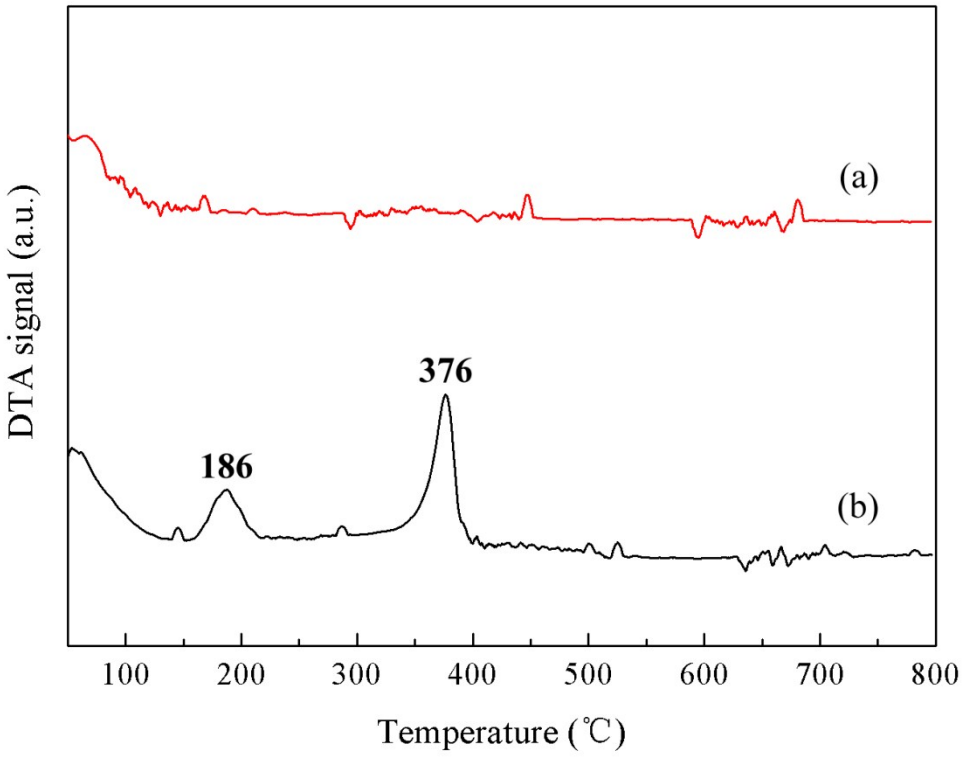

Fig. 10. FT-IR spectra of the catalyst samples: (a) fresh Fe-ZSM-5 zeolite membrane catalyst (b) used Fe-ZSM-5 zeolite membrane catalyst (8 hours) and (c) used Fe-ZSM-5 zeolite membrane catalyst (40 hours), respectively.

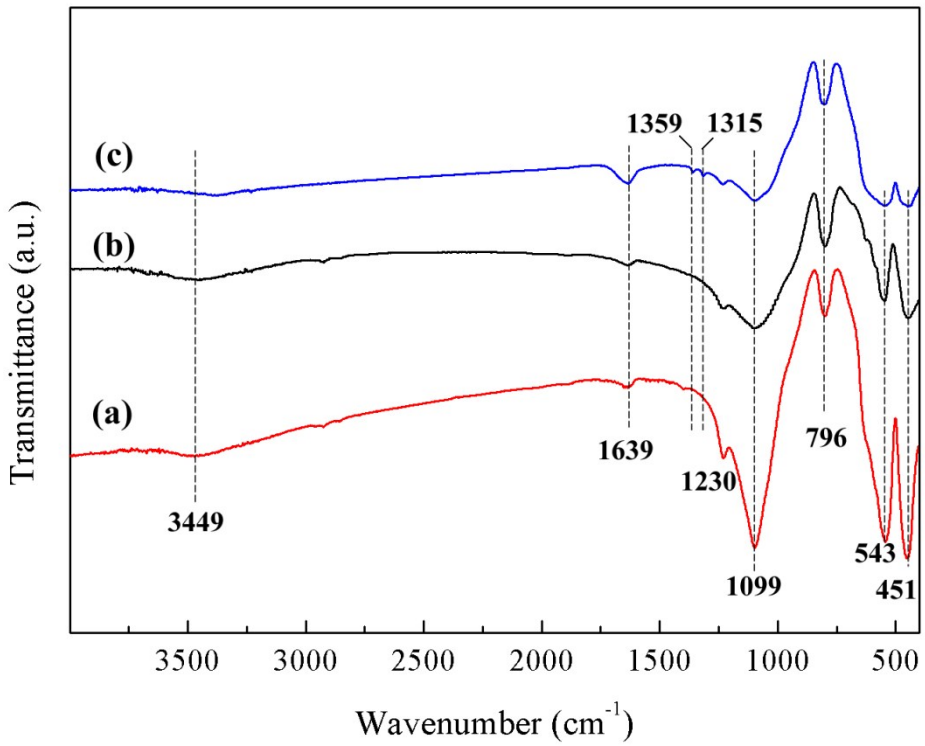

Fig. 11. Raman spectra of catalyst samples: (a) fresh Fe-ZSM-5 zeolite membrane catalyst, and (b) used Fe-ZSM-5 zeolite membrane catalyst, respectively.

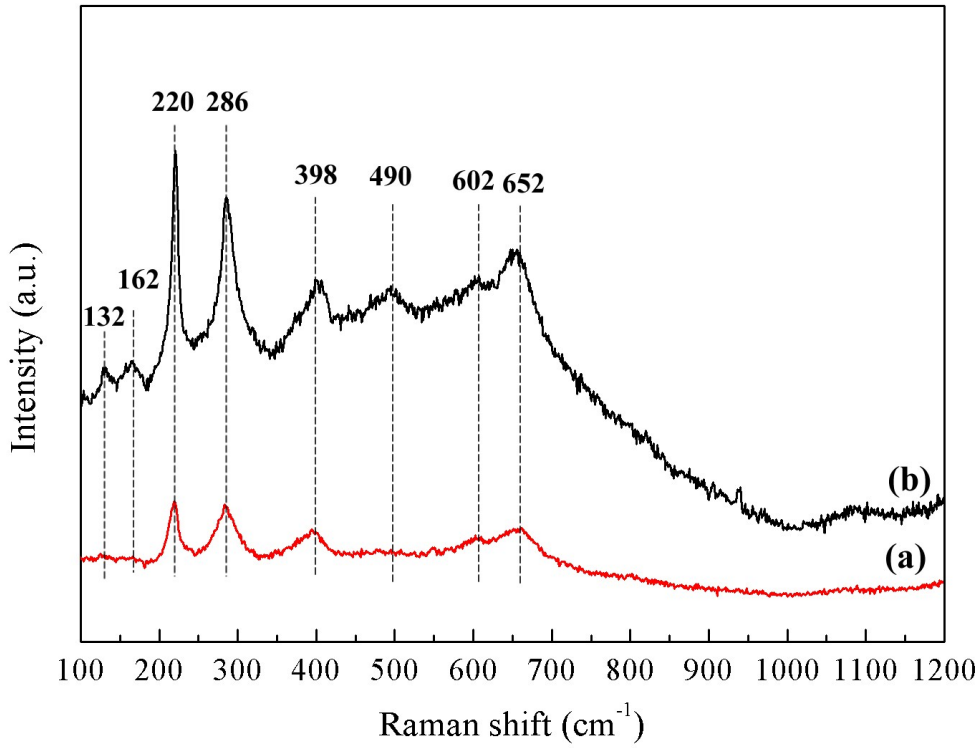

Graphical Abstract: